

Gaussian process modeling in approximate Bayesian computation to estimate horizontal gene transfer in bacteria

Marko Järvenpää¹, Michael U. Gutmann², Aki Vehtari¹, and Pekka Marttinen¹

¹Helsinki Institute for Information Technology HIIT, Department of Computer Science, Aalto University

²School of Informatics, University of Edinburgh

July 11, 2022

Abstract

Approximate Bayesian computation (ABC) can be used for model fitting when the likelihood function is intractable but simulating from the model is feasible. However, even a single evaluation of a complex model may take several hours, limiting the number of model evaluations available. Modeling the discrepancy between the simulated and observed data using a Gaussian process (GP) can be used to reduce the number of model evaluations required by ABC, but the sensitivity of this approach to a specific GP formulation has not been thoroughly investigated. We begin with a comprehensive empirical evaluation of using GPs in ABC, including various transformations of the discrepancies and two novel GP formulations. Our results indicate the choice of GP may significantly affect the accuracy of the estimated posterior distribution. Selection of an appropriate GP model is thus important. We define expected utility to measure the accuracy of classifying discrepancies below or above the ABC threshold, and show that by using this utility, the GP model selection step can be made automatic. Finally, based on the understanding gained with toy examples, we fit a population genetic model for bacteria, providing insight into horizontal gene transfer events within the population and from external origins.

Keywords: approximate Bayesian computation, intractable likelihood, Gaussian processes, input-dependent noise, model selection

1 Introduction

Estimating parameters of a statistical model often requires evaluating the likelihood function. For complex models, such as those arising in population genetics, deriving or evaluating the likelihood may be impossible. On the other hand, generating data from the model may be relatively straightforward. Approximate Bayesian Computation (ABC) [Beaumont et al., 2002, Hartig et al., 2011, Marin et al., 2012, Turner and Van Zandt, 2012] is an inference framework for such models. It is based on generating data from the simulation model for various parameter values and comparing the simulated data with the observed data using some discrepancy measure. The simplest ABC algorithm is the rejection sampler, which, at each step, randomly simulates a parameter from the prior distribution, runs the simulation model with this parameter, and finally accepts the parameter if the discrepancy between the simulated and observed data is smaller than some threshold. These steps are repeated until a sufficient number of samples from the approximate posterior have been collected. Many extensions for the ABC rejection sampler exist, for example Marjoram et al. [2003] presents a Markov Chain Monte Carlo approach for ABC.

One challenge in ABC is the choice of the discrepancy, which is usually defined using some representative summaries of the data, see e.g. Fearnhead and Prangle [2012], Blum et al. [2013]. Another challenge is

the selection of the ABC threshold ε , which can be interpreted as additional measurement or model error [Wilkinson, 2013]. The posterior density at parameter θ is then proportional to the probability that the discrepancy falls below the threshold. Too large a threshold may overestimate posterior uncertainty, whereas too small a value requires a lot of model evaluations due to the large rejection probability. Furthermore, several sequential algorithms have been proposed by Sisson et al. [2007], Beaumont et al. [2009], Toni et al. [2009], where the threshold is decreased at each step and samples from the previous step are used to form a new proposal. These methods thus attempt to focus model simulations mostly on the area with significant posterior probability. Related work has focused on setting the threshold adaptively [Moral et al., 2012, Lenormand et al., 2013].

An alternative to sampling is to construct an explicit approximation to the likelihood function, to be used as a proxy for the exact likelihood in, e.g., conventional MCMC samplers [Bornn et al., 2016]. In a method called synthetic likelihood the distribution of summary statistics is approximated with a multivariate Gaussian whose mean and covariance are estimated for each proposed parameter value by multiple evaluations at that point [Wood, 2010], see also Fan et al. [2013] for an alternative. Nonparametric approximations using kernel density estimates have also been considered [Blum, 2010, Turner and Sederberg, 2014], and connections between these and other approaches are discussed in detail by Drovandi et al. [2015b], Gutmann and Corander [2016]. Further assumptions about the shape or smoothness of the likelihood function as well as efficient schemes to select points to evaluate can yield computational improvements, and Gaussian processes [Rasmussen and Williams, 2006] (GPs) have been used in ABC to encode such assumptions. GPs were used by Drovandi et al. [2015a] to accelerate pseudo-marginal MCMC methods. Wilkinson [2014] modeled the likelihood function with a GP, and ruled out regions of the parameter space with negligible likelihood. An alternative is to model the individual summaries with a GP [Meeds and Welling, 2014, Jabot et al., 2014]. Gutmann and Corander [2016] used GPs in Bayesian optimization [Brochu et al., 2010, Shahriari et al., 2015] to efficiently decide parameter values where to simulate the model.

Typically hundreds of thousands of model simulations are needed for ABC inference, but in this article we focus on the challenging case where less than a thousand evaluations are available due to computational constraints. We adopt the BOLFI approach [Gutmann and Corander, 2016] where the discrepancy between observed and simulated data is modeled with a GP. This method has the advantage that computing the estimate even with relatively few model evaluations is possible, by avoiding the need to repeat the simulation many times for each possible parameter value. From the fitted GP, the posterior approximation can be computed analytically. The other main idea in BOLFI is to use Bayesian optimization to rapidly locate the posterior modal area. A potential issue in using a standard GP to model the discrepancies is that, in practice, the assumptions of this GP model may not hold [Gutmann and Corander, 2016]. For example, the discrepancy distribution may not be Gaussian or the variance may not be constant over the parameter space as assumed in the standard GP regression, causing error of unknown magnitude. In this article we study this issue in detail. To focus on the GP modeling aspect, we assume that the region of non-negligible posterior probability is known approximately in advance, for example it has been identified by Bayesian optimization, such that model evaluations from the interesting region can be carried out, although we acknowledge that detecting the region remains itself a topic of intensive ongoing research.

The impact of GP model assumptions on the resulting ABC posterior estimate in a realistic scenario is demonstrated in Figure 1, where different GP formulations are used to model the discrepancy distribution in the area with non-negligible posterior probability. The model here describes horizontal gene transfer between bacterial genomes, published recently by Marttinen et al. [2015]. The discrepancies were obtained by keeping the other parameters fixed to their respective point estimates, and generating realizations of the discrepancy with respect to a parameter that describes the frequency of horizontal gene transfer between bacterial strains in the population. The input-dependent noise model [Goldberg et al., 1997, Tolvanen et al., 2014] is able to take into account the heteroscedastic variance of the discrepancy and, while the true posterior is unavailable due to its intractable form and high computational cost of running the model, we assume that it consequently results in a good approximation to the posterior. On the other hand, with the standard GP regression the fit is poor, and the resulting posterior distribution seems clearly too wide. The square-root transformation to the discrepancy also seems to improve the fit.

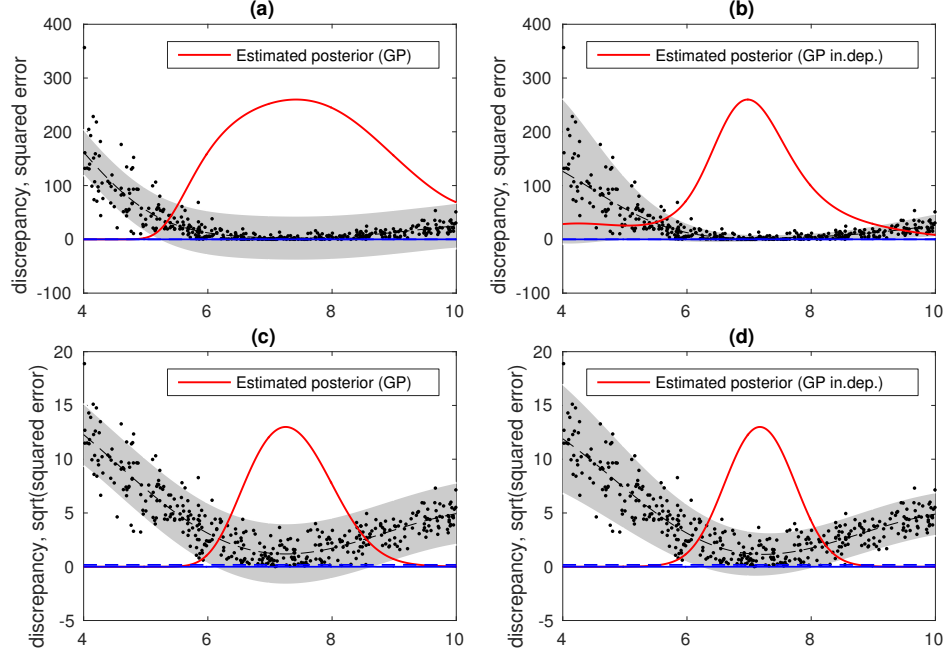


Figure 1: Good fit to the discrepancy data is obtained by using the input-dependent GP model and/or square-root transformation. x -axis shows the value of the simulation model parameter and y -axis the value of the (transformed) discrepancy. Black points are the simulated realizations of discrepancies, and the grey area is the 95% predictive interval, representing stochastic variation in the simulation. The red line shows the corresponding posterior approximation. In (a) the standard GP is fitted and its variance is clearly overestimated in the posterior modal area, likely yielding a poor approximation to the posterior. Using input-dependent GP model as in (b) or transforming the discrepancy as in (c) result in better approximations. The best fit is obtained when using both the transformation and the input-dependent GP model in (d), as even after the square-root transformation the variance of the discrepancy is not constant.

Our paper makes the following contributions:

- Motivated by the preliminary investigation with the population genetics model discussed above, we assess the impact of the GP modeling used in ABC on the inferences obtained for multiple benchmark models. We find that no GP model is uniformly superior to others.
- We propose two generalizations of previously presented GP-ABC approaches: first, we allow heteroscedastic noise in the GP; second, we use a classifier GP to directly model the probability of the discrepancy being below the ABC threshold.
- We propose a new utility function to automate GP model choice for ABC. The utility function favours models that achieve higher accuracy in classifying discrepancies below or above the ABC threshold.
- As a practical application, we derive an accurate posterior distribution for the population genetic model for gene transfer in bacteria, allowing us to make inferences about the relationship between gene deletions and introductions, and between gene transfers from within the population and from external origins.

This paper is organized as follows. In Section 2 we review general ABC and BOLFI methods and introduce different GP models that can be used for the BOLFI approach. We also discuss GP model selection in ABC. In Section 3 we present findings from multiple example problems to illustrate the impact of GP assumptions

and model selection in ABC, and finally present the results for the bacterial genomics model. Section 4 contains discussion and in Section 5 we conclude with our recommendations for ABC inference when the number of model evaluations is extremely limited.

2 Background and methods

2.1 ABC

We assume that we have observed data $\mathbf{y} \in \mathbb{R}^d$ from the simulation model whose likelihood function can be written as $p(\mathbf{y} | \boldsymbol{\theta})$, where the unknown parameters to be estimated are $\boldsymbol{\theta} \in \Theta \subset \mathbb{R}^p$. The prior information is modeled with prior density $p(\boldsymbol{\theta})$. The posterior distribution can then be computed from the Bayes' theorem

$$p(\boldsymbol{\theta} | \mathbf{y}) = \frac{p(\boldsymbol{\theta})p(\mathbf{y} | \boldsymbol{\theta})}{p(\mathbf{y})} \propto p(\boldsymbol{\theta})p(\mathbf{y} | \boldsymbol{\theta}),$$

where the normalization factor is $p(\mathbf{y}) = \int p(\boldsymbol{\theta})p(\mathbf{y} | \boldsymbol{\theta}) d\boldsymbol{\theta}$.

When either the analytic form of the likelihood function $p(\mathbf{y} | \boldsymbol{\theta})$ is unavailable or its values cannot be evaluated in a reasonable computation time, the standard alternative is to use approximate Bayesian computation (ABC) [Beaumont et al., 2002, Hartig et al., 2011, Marin et al., 2012, Turner and Van Zandt, 2012]. The ABC targets the approximate posterior

$$p_{\text{ABC}}(\boldsymbol{\theta} | \mathbf{y}) \propto p(\boldsymbol{\theta}) \int p_{\varepsilon}(\mathbf{y} | \mathbf{x})p(\mathbf{x} | \boldsymbol{\theta}) d\mathbf{x},$$

where $\mathbf{x} \in \mathbb{R}^d$ denotes pseudo-data generated by the simulation model with parameter $\boldsymbol{\theta}$. The pseudo-data \mathbf{x} are compared to the observed data \mathbf{y} using a probability distribution $p_{\varepsilon}(\mathbf{y} | \mathbf{x})$. Typically a uniform kernel is used so that $p_{\varepsilon}(\mathbf{y} | \mathbf{x}) \propto \mathbb{1}_{d(\mathbf{y}, \mathbf{x}) \leq \varepsilon}$, where $d(\cdot, \cdot)$ is a discrepancy function between the two data sets and ε denotes the threshold that, in practice, represents the tradeoff between estimation accuracy and computational efficiency. The discrepancy is often formed using some summary statistics such that if s is a mapping from the data space \mathbb{R}^d to a lower dimensional space of the summary statistics, then $d(\mathbf{y}, \mathbf{x}) = d(s(\mathbf{y}), s(\mathbf{x}))$. Choosing informative summaries and combining them in a reasonable way affect the resulting approximate posterior (see e.g. Marin et al. [2012]), but we do not consider this problem here.

Given N samples generated from the simulation model with a chosen parameter $\boldsymbol{\theta}$, so that $\mathbf{x}_{\boldsymbol{\theta}}^{(i)} \sim p(\mathbf{x} | \boldsymbol{\theta})$, $i = 1, \dots, N$, the (unnormalized) ABC posterior at $\boldsymbol{\theta}$ can be estimated using

$$p_{\text{ABC}}(\boldsymbol{\theta} | \mathbf{y}) \propto p(\boldsymbol{\theta}) \sum_{i=1}^N p_{\varepsilon}(\mathbf{y} | \mathbf{x}_{\boldsymbol{\theta}}^{(i)}).$$

Alternatively, one can use ABC rejection sampling to sample from the ABC posterior. This algorithm consists of the following steps:

1. Draw $\boldsymbol{\theta}^{(i)} \sim p(\boldsymbol{\theta})$
2. Generate $\mathbf{x}^{(i)} \sim p(\mathbf{x} | \boldsymbol{\theta}^{(i)})$ from the simulation model and compute the weight $\omega^{(i)} = p_{\varepsilon}(\mathbf{y} | \mathbf{x}^{(i)})$
3. Stop when enough samples have been generated.

The resulting weighted samples $\{(\boldsymbol{\theta}^{(i)}, \omega^{(i)})\}$ are then generated from the ABC-posterior. If the uniform kernel is used, then the weights are either 0 or 1 describing whether the realized discrepancies are above or below the threshold.

2.2 BOLFI method

To speed up computations, Gutmann and Corander [2016] proposed a method named BOLFI, which builds a model of the discrepancy $d_{\boldsymbol{\theta}} = d(\mathbf{y}, \mathbf{x}_{\boldsymbol{\theta}})$ between the observed data \mathbf{y} and the simulated data $\mathbf{x}_{\boldsymbol{\theta}}$, and focuses computations on the modal area of the likelihood using Bayesian optimization. BOLFI can be used to

obtain point estimates as well as full posteriors. A point estimate for the parameter of the simulation model can be computed as the value minimizing the expected discrepancy between observed and simulated data, $\hat{\theta} = \arg \min_{\theta \in \Theta} \mathbb{E}(d_{\theta})$. The expectation can in practice be estimated by simulating multiple realizations of the discrepancy from the simulation model for each required parameter θ . However, a better alternative is to model the discrepancy using a GP and minimize the estimated GP mean curve. This approach makes it unnecessary to repeat the simulation multiple times with each parameter value proposed.

The fitted GP model can be used for computing the full posterior of the simulation model. An estimate of the (unnormalized) likelihood can be obtained as $\mathbb{P}(d_{\theta} \leq \varepsilon)$, where the probability is computed using the statistical model (i.e. the fitted GP) for the discrepancy as a function of the parameter θ . Technically, if the mean and variance estimates from the GP are given by $\mu_t(\theta)$ and $v_t(\theta)$, respectively, then the likelihood estimate at θ is proportional to $\Phi((\varepsilon - \mu_t(\theta))/\sqrt{v_t(\theta)})$, where ε is the threshold and Φ is the cumulative distribution function of the standard Gaussian distribution. Finally, an estimate of the posterior density can be obtained by multiplying the estimated likelihood with the prior density $p(\theta)$.

In BOLFI, the parameter values $\theta_i, i = 1, \dots, t$, to run the simulation with, are adaptively focused around the posterior mode (*exploitation*), allowing some *exploration* further away from the mode. Originally, such Bayesian optimization strategies were designed for minimizing functions. In BOLFI, a stochastic extension of the commonly used upper confidence bound criterion for deciding which points to run was presented, to prevent evaluations from being too tightly concentrated around the mode. Sequential history matching has also been investigated for adaptively constructing evaluation points [Wilkinson, 2014, Holden et al., 2015]. However, these works focus on modeling the likelihood or log likelihood with a GP, whereas here and in BOLFI the goal is to model the discrepancies. Here we assume the location of the posterior mode to be known approximately, and generate the training data uniformly around the mode, thus allowing us to focus on the aspect of modeling the discrepancies with a GP.

2.3 GP models for GP-ABC

In this article we investigate the accuracy of the posterior approximation when the standard GP is used to model the discrepancy [Gutmann and Corander, 2016]. In addition, we include two novel extensions (see below) of earlier GP-ABC approaches in our comparison: the input-dependent GP and the classifier GP. We assume that training data of discrepancy-parameter pairs $D_t = \{(d(\theta_i), \theta_i)\}_{i=1}^t$ is available and aim to model the discrepancy and the resulting posterior as accurately as possible using D_t . GPstuff 4.6 [Vanhatalo et al., 2013] is used for fitting the GP models. The hyperparameters of all models are learned by maximizing the marginal likelihood, see Rasmussen and Williams [2006]. For the input-dependent GP and classifier GP, Laplace approximation is used. We also experimented with the expectation propagation approximation, derived by Tolvanen et al. [2014] for the input-dependent GP model, but this came at additional cost and results were qualitatively similar.

In the **standard GP regression** one assumes that $d_{\theta} \sim \mathcal{N}(f(\theta), \sigma^2)$ and $f(\theta) \sim \mathcal{GP}(m(\theta), k(\theta, \theta'))$ with a mean function $m : \Theta \rightarrow \mathbb{R}$ and covariance function $k : \Theta \times \Theta \rightarrow \mathbb{R}$. We set $m(\theta) = 0$, unlike Wilkinson [2014], Gutmann and Corander [2016], who assumed that the discrepancy goes to infinity far from the minimum, and thus included quadratic terms to the mean function. However, in this article we do not make these assumptions, which allows for estimating posterior distributions of arbitrary shapes, at the cost of potentially overestimating the tail area probability. We use the squared exponential covariance function $k(\theta, \theta') = \sigma_f^2 \exp(-\sum_{i=1}^p (\theta_i - \theta'_i)^2 / (2l_i^2))$. Given the hyperparameters σ_f^2, l_i and σ^2 , estimated by maximizing the marginal likelihood, and training data D_t , the mean and variance curves can be computed as in Rasmussen and Williams [2006].

Next we describe the **input-dependent GP model** [Goldberg et al., 1997, Tolvanen et al., 2014]. In the standard GP model the noise variance describing the randomness in the discrepancy due to the stochastic simulation model is assumed constant. We relax this by assuming $d_{\theta} \sim \mathcal{N}(f(\theta), \sigma^2 \exp(g(\theta)))$, $f(\theta) \sim \mathcal{GP}(m(\theta), k(\theta, \theta'))$ and $g(\theta) \sim \mathcal{GP}(m_n(\theta), k_n(\theta, \theta'))$. That is, also the variance of the discrepancy is modeled with a GP allowing it to change smoothly as a function of the parameter θ . Since the variance must be positive, the logarithm of the variance is modeled with the GP. As before we set $m(\theta) = 0$, and also

$m_n(\boldsymbol{\theta}) = 0$, implying that a priori the average variance is close to σ^2 . We use the squared exponential covariance functions $k(\boldsymbol{\theta}, \boldsymbol{\theta}') = \sigma_f^2 \exp\left(-\sum_{i=1}^p (\theta_i - \theta'_i)^2 / (2l_{f_i}^2)\right)$ and $k_n(\boldsymbol{\theta}, \boldsymbol{\theta}') = \sigma_g^2 \exp\left(-\sum_{i=1}^p (\theta_i - \theta'_i)^2 / (2l_{g_i}^2)\right)$. There are $2p + 2$ hyperparameters to be estimated: p lengthscale parameters, l_{g_i} , l_{f_i} , and one signal variance parameter for each covariance function, σ_f^2 , σ_g^2 . The value of σ^2 is fixed to make the hyperparameters of the covariance function identifiable.

The GP models above can be used for modeling the ABC discrepancy between observed and simulated data. However, for computing the approximate posterior, it is sufficient to know the probability that the discrepancy is below the threshold ε . Motivated by this, we propose a new method which we call the **classifier GP** in which the lower tail probability is directly modeled as a function of the parameter $\boldsymbol{\theta}$ using GP binary classification. We interpret the observations $z_i = 2\mathbb{1}_{d_i \leq \varepsilon} - 1$ as class labels $+1$ and -1 such that $p(z_i | f(\theta_i)) = g^{-1}(z_i f(\theta_i))$, where g is either the logit or probit link function and $f(\boldsymbol{\theta}) \sim \mathcal{GP}(m(\boldsymbol{\theta}), k(\boldsymbol{\theta}, \boldsymbol{\theta}'))$. Hence, unlike the GP models above, this corresponds to an assumption that the discriminative function is a smooth curve, but does not make assumptions about the distribution of the discrepancy. For each parameter value $\boldsymbol{\theta}$ the model thus specifies the probability of the discrepancy being classified as $+1$, i.e., to be below the threshold. We use the logit link in our experiments as the difference to probit was minor. Unlike with other GP models, we add an additional constant to the prior mean function $m(\boldsymbol{\theta})$ to take into account the fact that the tail probabilities are generally very small. Without this modification, the discriminative function tended to become nonzero near the parameter bounds, inducing posterior mass near the boundaries, and, consequently, poor approximations. We chose the squared exponential covariance function for the latent function f as for the standard GP method. A potential drawback is that the threshold must be selected before fitting the model because the discrepancies must be transformed to class labels z_i , and, thus, comparing multiple thresholds may be slow.

2.4 GP model selection

Since the distribution of the discrepancy depends on the characteristics of the simulation model and the chosen discrepancy, some GP models will fit better than others to the discrepancy data. This gives the motivation to consider model selection, to guide the selection of the GP in practice. While there exist various normality tests for assessing whether the Gaussian assumption of the GP model holds, they are difficult to apply in our case because typically only a single evaluation is available for each parameter value in D_t . Consequently, we propose two utility functions for comparing the GP models, with the aim of choosing the GP model that yields the most accurate estimate of the posterior. See, e.g., Bernardo and Smith [2001] for a thorough discussion on using expected utility for model selection.

As the first criterion, we consider the expected log predictive density for a new discrepancy value $d^{(t+h)}$ evaluated at some future evaluation point $\boldsymbol{\theta}^{(t+h)}$ for $h = 1, 2, \dots$. Here the utility of a single observation $d^{(t+h)}$ is defined by

$$u_h = \log p(d^{(t+h)} | \boldsymbol{\theta}^{(t+h)}, D^{(1:t)}, M),$$

where $D^{(1:t)} = \{(d^{(i)}, \boldsymbol{\theta}^{(i)})\}_{i=1}^t$ denotes the data gathered thus far and M denotes the chosen model. The different transformations of the discrepancy can be taken into account by considering the effect of the transformation g so that $d' = g(d)$. The expected utility estimate is then obtained by averaging over all the possible realizations of the future data yielding $\bar{u} = \mathbb{E}(u_h)$. This utility measures how well the GP predicts the distribution of the discrepancies, which is used for computing the posterior estimate of the simulation model. As we do not know the distribution of the discrepancy-parameter data $(d^{(t+h)}, \boldsymbol{\theta}^{(t+h)})$, we approximate the expected utilities using the data gathered thus far $D^{(1:t)}$ [Vehtari and Lampinen, 2002]. Assuming the future data have the same distribution as the training data, we can replace the expectation with an average, which gives

$$\bar{u}_{\text{train}} = \frac{1}{t} \sum_{i=1}^t \log p(d^{(i)} | \boldsymbol{\theta}^{(i)}, D^{(1:t)}, M).$$

However, here the same data are used both for model fitting as well as to estimate the predictive performance,

and a better estimate is obtained by K -fold cross-validation (CV)

$$\bar{u}_{\text{CV}} = \frac{1}{t} \sum_{i=1}^t \log p(d^{(i)} | \boldsymbol{\theta}^{(i)}, D^{(1:t) \setminus s(i)}, M),$$

where the data are split into K (almost) equally sized groups and $s(i)$ denotes the indexes of the group to which the i th data point belongs. In practice, we use $K = 10$. In the sequel, we refer to this as the **mlpd utility**, which stands for the mean of the log-predictive density.

The downside of the mlpd utility is that it does not in any way acknowledge the final purpose for which the selected GP model will be used, i.e., to approximate the posterior distribution by computing the probability that, for a given parameter value, the simulated discrepancy is below the threshold. Consequently, it may give high scores to GP models which broadly model the discrepancy accurately, whereas the focus should be on how well the smallest discrepancies are modeled, as these are the ones that affect the posterior approximation most. Motivated by this, we frame the problem as a classification task which then leads to a new utility function tailored for the ABC inference. The utility for a single observation $d^{(t+h)}$ is defined by

$$u_h^c = \mathbb{1}_{d^{(t+h)} \leq \varepsilon} \log(\mathbb{P}(d^{(t+h)} \leq \varepsilon | M)) + \mathbb{1}_{d^{(t+h)} > \varepsilon} \log(\mathbb{P}(d^{(t+h)} > \varepsilon | M)),$$

where $\mathbb{P}(d^{(t+h)} \leq \varepsilon | M)$ is the probability that a new realization of the discrepancy $d^{(t+h)}$ at a test point $\boldsymbol{\theta}^{(t+h)}$ is smaller than the threshold ε according to model M (conditioning on $\boldsymbol{\theta}^{(t+h)}$ and $D^{(1:t)}$ is omitted to simplify notation). This utility penalizes realizations of the discrepancy that are under the threshold when, according to the model, this should happen only with a very small probability, or vice versa. An additional advantage of this utility is that it is invariant to transformation of the discrepancy if the threshold ε is transformed accordingly, and can be used also to compare the classifier GP to other models, as it only requires the probability that a discrepancy is below the threshold, and not the full distribution. Again, we use the K -fold CV with $K = 10$ to approximate the expected utility, so that

$$\bar{u}_{\text{CV}}^c = \frac{1}{t} \sum_{i=1}^t (\mathbb{1}_{d^{(i)} \leq \varepsilon} \log(\mathbb{P}(d^{(i)} \leq \varepsilon | D^{(1:t) \setminus s(i)}, M)) + \mathbb{1}_{d^{(i)} > \varepsilon} \log(\mathbb{P}(d^{(i)} > \varepsilon | D^{(1:t) \setminus s(i)}, M))).$$

We call this the **classifier utility** from now on.

Naturally, also other utility functions could be considered. A sensible alternative would be to give the evaluation points different weights, reflecting their importance in posterior inference. It remains to be studied how model comparison could be used as part of a Bayesian optimization algorithm, to select points where to sample next. We note that these methods might be theoretically problematic because the next evaluation points $\boldsymbol{\theta}^{(t+h)}$ would depend on the previously fitted GP model, and consequently, the distribution of the future evaluation points would be different for different GP choices.

3 Results

3.1 Toy examples

We consider several one and two-dimensional toy examples to study the approximation error for different GP models and transformations of the discrepancy. A summary of the test problems is given in Table 1. Although simple, these examples highlight potential challenges in modeling the discrepancy that we expect carry over to many realistic problems of potentially higher dimensionality. The estimated posterior curves are compared to the true ones, available analytically for the examples. Sufficient statistics are used to compute the discrepancies, except for the Lotka-Volterra (LV) model, see Example 3.4 below. Total variation (TV) is used as the criterion for the quality of posterior approximation i.e. $\text{TV}(p_{\text{true}}, p_{\text{approx}}) = 1/2 \int_{\Theta} |p_{\text{true}}(\boldsymbol{\theta}) - p_{\text{approx}}(\boldsymbol{\theta})| d\boldsymbol{\theta}$. Values for this integral are computed numerically. We also consider the Kullback-Leibler divergence (KL), defined as $\text{KL}(p_{\text{true}} || p_{\text{approx}}) = \int_{\Theta} p_{\text{true}}(\boldsymbol{\theta}) \log(p_{\text{true}}(\boldsymbol{\theta})/p_{\text{approx}}(\boldsymbol{\theta})) d\boldsymbol{\theta}$, which is also computed numerically.

Test problem and model	prior	n	squared discrepancy	true θ
Gaussian 1, $\mathcal{N}(\theta, 1)$	$\mathcal{U}([-5, 5]), \mathcal{U}([-0.5, 3])$	10	$(\bar{y} - \bar{y}(\theta))^2$	1
Bimodal, $\mathcal{N}(\theta^2, 2)$	$\mathcal{U}([-5, 5]), \mathcal{U}([-2.5, 2.5])$	5	$(\bar{y} - \bar{y}(\theta))^2$	± 1
Gaussian 2, $\mathcal{N}(0, \theta)$	$\mathcal{U}([0, 10]), \mathcal{U}([0, 5])$	10	$(\sigma_y^2 - \sigma_{y(\theta)}^2)^2$	1
Poisson, $\text{Poi}(\theta)$	$\mathcal{U}([0, 10]), \mathcal{U}([0, 5])$	10	$(\bar{y} - \bar{y}(\theta))^2$	2
GM 1, $\mathcal{GM}(0.65, \theta, \theta + 5, 1, 2)$	$\mathcal{U}([-15, 15]), \mathcal{U}([-10, 5])$	1	$(y_1 - y_1(\theta))^2$	1
GM 2, $\mathcal{GM}(0.7, \theta, \theta, 3, 0.25)$	$\mathcal{U}([-15, 15]), \mathcal{U}([-6, 6])$	1	$(y_1 - y_1(\theta))^2$	1
Uniform, $\mathcal{U}([0, \theta])$	$\mathcal{U}([0, 10]), \mathcal{U}([0, 5])$	5	$(\max\{y_i\} - \max\{y_i(\theta)\})^2$	2
2D Gaussian 1, $\mathcal{N}(\theta, \Sigma)$	$\mathcal{U}([1.5, 4] \times [1.5, 4])$	10	$(\bar{\mathbf{y}} - \bar{\mathbf{y}}(\theta))^T \Sigma^{-1} (\bar{\mathbf{y}} - \bar{\mathbf{y}}(\theta))$	$[2.5, 2.5]^T$
2D Gaussian 2, $\mathcal{N}(\theta_1, \theta_2)$	$\mathcal{U}([2, 4.5] \times [0.5, 5])$	25	$(\bar{y} - \bar{y}(\theta))^2 + (\sigma_y^2 - \sigma_{y(\theta)}^2)^2$	$[3, 2]^T$
Lotka-Volterra, see the text	$\mathcal{U}([0.25, 1.25] \times [0.5, 1.5])$	8	see the text	$[1, 1]^T$

Table 1: Description of the test problems. Above, \bar{y} denotes the sample mean of $\{y_i\}_{i=1}^n$ and, similarly, σ_y^2 is the sample variance. The data points $y_i(\theta)$ are independent and identically distributed draws from the simulation model with parameter θ . Also, $\mathcal{GM}(\alpha, \mu_1, \mu_2, \sigma_1^2, \sigma_2^2) = \alpha \mathcal{N}(\mu_1, \sigma_1^2) + (1 - \alpha) \mathcal{N}(\mu_2, \sigma_2^2)$. For the 2D Gaussian we use a fixed covariance matrix Σ with unit covariances and correlation 0.5. For some examples the prior column contains two alternative prior distributions that were tested. For the description of the Lotka-Volterra model, see the text.

We use uniform priors for the parameters of the simulation models over a range covering the modal area of the true posterior. We repeat the experiments also with a much wider support (see Table 1), although this is less relevant in practice, when the goal is to obtain an accurate posterior estimate where the majority of mass is located, and hence focus most simulations there. We note that the use of other priors, as well as adaptive schemes for choosing the training data would be possible too [Gutmann and Corander, 2016].

We consider two transformations of the squared discrepancy, abbreviated as *se*, namely, the log and the square-root transformations (*log* and *sqr*t). Although other transformations could be considered, the ones chosen already demonstrate how the model selection criteria work in practice and illustrate the fact that the transformed discrepancy may be easier to model. We note that instead of transforming the whole discrepancy one could transform the individual summaries before combining them to a discrepancy function, but we do not consider this here. Also, we set the ABC threshold ε customarily to be the 0.05th quantile of the sampled discrepancies, unless stated otherwise, and use the same threshold for all GP-ABC methods as well as the ABC rejection sampler, which we include to compare with a standard ABC algorithm. We improve the basic ABC rejection sampler by using kernel density estimation to approximate the posterior curve from the accepted samples, thereby imposing basic smoothness assumptions of the posterior as a post-processing step. From now on, we call this smoothed version of the ABC rejection sampler simply rejection ABC.

Below we analyze in detail some of the test problems. Since any particular result depends on the realization of a stochastic model, we repeat the computations 100 times to obtain estimates of the bias and variance of the estimator for the posterior curve. The full summary of these results is gathered in Tables 2 and 3.

Example 3.1 (Gaussian 1). We consider a simple Gaussian model with an unknown mean and known variance as the first example, see 'Gaussian 1' in Table 1. We first analyze it analytically. Consider the discrepancies $d_\theta^2 = (\bar{y} - \bar{x}_\theta)^2$ and $d_\theta = |\bar{y} - \bar{x}_\theta|$. Using basic properties of the expectation and the Gaussian distribution, we obtain $\mathbb{E}(d_\theta^2) = (\theta - \bar{y})^2 + \sigma^2/n$ and $\text{var}(d_\theta^2) = 2\sigma^2(2(\theta - \bar{y})^2 + 1)/n$. Similarly $\text{var}(d_\theta) \approx \sigma^2/n$, which holds accurately for a large $|\theta|$. We see that the variance of the discrepancy can depend on θ . In particular, in the case of the squared discrepancy d_θ^2 , the variance grows quadratically as a function on the parameter θ . However, with d_θ the variance is approximately constant, at least outside the modal region.

The main observations of this example are illustrated in Figure 2. In (a-c) a prior over a wide range is used and in (d-f) training data are gathered only within a narrow region around the posterior mode.

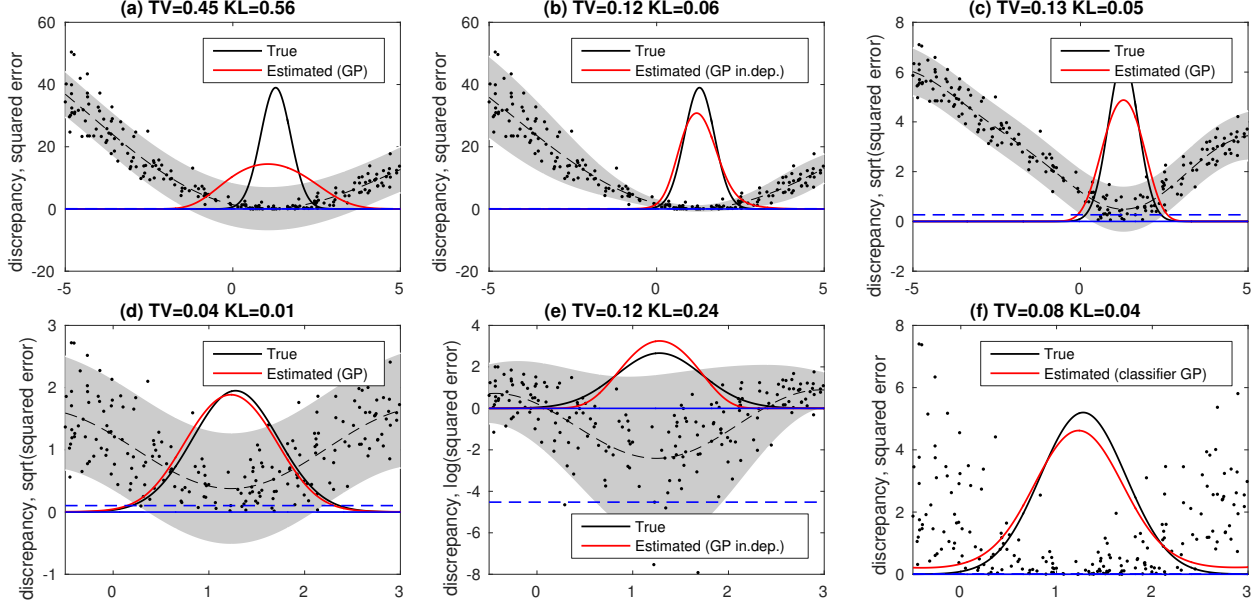


Figure 2: Results for the 'Gaussian 1' model. The grey area is the 95% probability interval, blue dashed line is the threshold and the black dots represent realizations of the discrepancy. In (a) the GP is fitted to squared discrepancy realizations on a wide interval resulting in a poor approximation. Better approximations are obtained by the input-dependent GP model (b) or transforming the discrepancy (c). In (d) the fitting is done on the area of significant posterior mass resulting in the best fit in terms of both TV and KL, even if the variance of the discrepancy is still clearly overestimated in the modal region. In (e) the posterior uncertainty is slightly underestimated due to the skewness of the log-transformed discrepancy. The classifier GP in (f) slightly overestimates the tails of the posterior. While the classifier GP yields a good approximation in this particular case, on average it did not perform as well as some other GP-based methods, see Table 2.

Comparing (a) and (b) shows that the input-dependent GP model yields a much better approximation than the standard GP. In (a) the posterior is inflated not only due to the nonzero threshold but also because of a poor GP fit, which can not be corrected by increasing the number of simulations. Furthermore, different transformations change the behaviour of the discrepancy. In the square-root -transformed case (c), the variance of the discrepancy is approximately constant, and the standard GP yields a good approximation comparable to (b). The best approximation is obtained in (d) because the threshold can be set to a smaller value due to the larger number of small discrepancy realizations compared to (a-c). The threshold used here was the 0.05th quantile of the realizations; however, similar conclusions hold for the 0.01th quantile.

Example 3.2 (Poisson). Here, we consider estimating the parameter of the Poisson distribution which demonstrates the benefit of GP modeling compared to the rejection ABC. Figure 3 shows typical results. Here the data have discrete values but the discrepancy is approximately Gaussian, and the variance of the discrepancy grows as a function of the parameter. The input-dependent model does not improve the results visibly, even if the fit to the discrepancy data is evidently better. However, when the upper limit of the parameter range is increased, the input-dependent GP model starts to outperform the standard GP (not shown). The best approximations are obtained when the square-root transformation is used as in (a-b) since then the discrepancy is approximately Gaussian, although its variance is not constant. The rejection ABC does not work very well compared to the GP models, as seen in (c).

Example 3.3 (GM 1). The third example demonstrates that both the standard and input-dependent GP models may fail to capture the bimodal shape of the posterior. Here also the discrepancy distribution is bimodal conditional on specific parameter values. A particular realization is shown in Figure 4. The GP

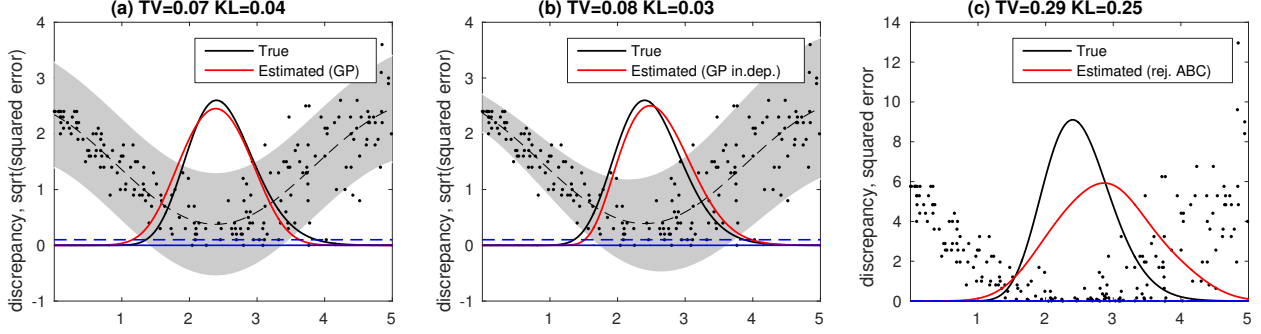


Figure 3: Results for the 'Poisson' example, demonstrating the benefits of the GP modeling. The input-dependent GP model (b) fits the discrepancy data better than the standard GP (a). Despite this difference, the posterior approximations are about equally good. The rejection ABC (c) yields a less accurate approximation with only the 200 training points available.

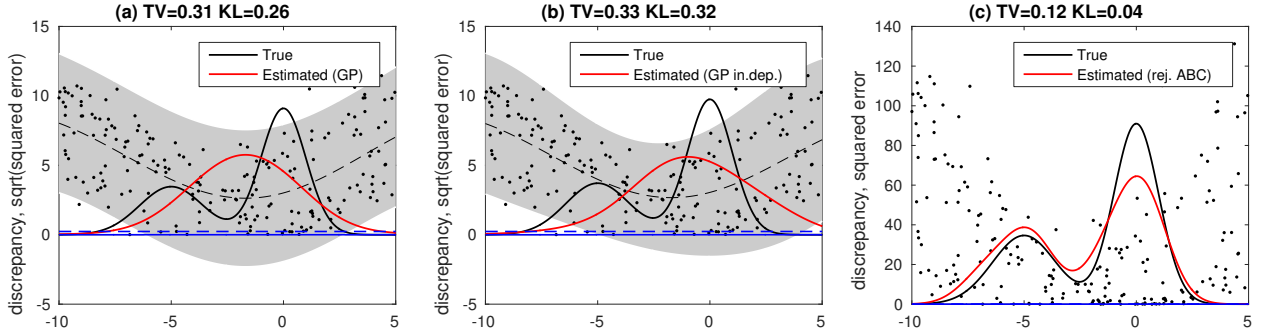


Figure 4: Neither the standard (a) nor the input-dependent GP model (b) learn the shape of the posterior in the bimodal 'GM 1' example. Notably, not only the posterior, but also the discrepancy distribution, given a particular parameter value, is bimodal, which is the explanation of this behaviour. 200 points were generated from the model, but similar results were obtained with a larger set of simulations, and with other transformations. On the other hand, the rejection ABC (c), which does not assume the Gaussianity of the discrepancy, uncovers the bimodal shape.

and input-dependent GP yield slightly different approximations, neither of which captures the bimodality. However, fixing the lengthscale to a small value allows to capture the bimodal shape but with the cost of making the overall shape of the estimated posterior wiggly (not shown). The rejection ABC works here better even with the limited training set size of 200.

The above observations do not hold for all bimodal posteriors. Namely, we designed another such toy problem where the posterior is bimodal, the 'Bimodal' in Table 1. In contrary to the Gaussian mixture model above, the distribution of the discrepancy is close to a Gaussian for any parameter. The bimodality of the posterior occurs because the discrepancy tends to get small values near the true parameter values -1 and 1 and larger values elsewhere. This type of discrepancy can be modeled well, and consequently, the bimodal shape of the posterior can also be learnt accurately (exact results not shown).

Example 3.4 (Lotka-Volterra). We consider the Lotka-Volterra model, used e.g. by Toni et al. [2009] to compare ABC methods, describing the evolution of prey and predator populations, defined by differential equations

$$\frac{dx_1}{dt} = \theta_1 x_1 - x_1 x_2, \quad \frac{dx_2}{dt} = \theta_2 x_1 x_2 - x_2,$$

where $x_1 = x_1(t)$ and $x_2 = x_2(t)$ describe the prey and predator species at time t , respectively. Their initial

values are set to $x_1(0) = 0.5$ and $x_2(0) = 1.0$. Vector $\boldsymbol{\theta} = (\theta_1, \theta_2)$ contains the parameters to be estimated. The 8 measurements for (x_1, x_2) are corrupted by additive independent and identically distributed Gaussian noise $\mathcal{N}(0, 0.5^2)$ which is the only source of stochasticity. We considered the discrepancy

$$d^2(\boldsymbol{\theta}) = \sum_{i=1}^8 \sum_{j=1}^2 (x_j(t_i) - \hat{x}_j(t_i, \boldsymbol{\theta}))^2,$$

where $x_j(t_i)$ are the noisy measurements at time t_i and $\hat{x}_j(t_i, \boldsymbol{\theta})$ the corresponding predictions with the model given the parameters $\boldsymbol{\theta}$. The prior and the true value of the parameter vector are shown in Table 1. The exact posterior is analytically tractable as shown by Toni et al. [2009]. However, unlike with other toy models, we compare the results to an ABC posterior obtained by rejection sampling with 10^6 samples and the threshold ε chosen such that 1000 discrepancies are below ε . This approach is chosen because the true posterior clearly deviates from the exact ABC posterior, due to the lack of low-dimensional summary statistics and a small number of training data, making comparisons to the true posterior meaningless in our experimental setup.

The results are shown in Figure 5, and we see that the GP formulation has only a moderate impact. However, the squared discrepancy as well as the rejection ABC perform worse than the other methods, as seen also in Table 3. The rejection ABC also has a higher variance than the GP methods. Nevertheless, in all the cases the uncertainty is inflated, and it appears that many more evaluations allowing a smaller threshold or low-dimensional summaries would be needed to improve accuracy. We did not test the LV model with the wider prior support in detail. This was because the values of the discrepancy tended to grow very fast when moving away from the mode, which made fitting the GP models challenging, usually resulting in a very poor fit, and making comparisons meaningless.

Further comparisons between the GP models and transformations are shown in Tables 2 and 3. In general, whenever the discrepancy for a particular parameter value is close to a Gaussian, or if the number of evaluations is low such that only a few discrepancy values are below the threshold ε , the GP-based approaches yield better posterior approximations than the rejection ABC or classifier GP methods. However, if the Gaussian assumptions are violated, as in Example 3.3, the rejection ABC and the classifier GP are the more accurate. Increasing the number of simulations does not help since the model misspecification issue remains. Interestingly, as few as 50 model evaluations in 1D (200 in 2D) result in almost as accurate results as 400 evaluations in 1D (600 in 2D). On the other hand, the accuracies of the rejection-ABC and classifier GP clearly improve as the number of evaluation points is increased. Additional evaluations also improve the stability of GP estimation and, hence, decrease the variance in the results.

The classifier GP performs generally similarly or slightly better than the rejection ABC. In the 'Uniform' example, the classifier GP is clearly superior. This happens because the posterior is accumulated on the left boundary of the parameter range, which makes it challenging for the kernel density estimator of the rejection ABC to model. Generally, with a small number of evaluations, the error of the classifier GP is still large, but as the number of evaluations increases, the accuracy increases rapidly reaching and finally clearly outperforming the rejection ABC. However, decreasing the threshold to the 0.01th quantile leads to conservative results since the number of realizations of the discrepancy below the threshold becomes very small. Especially in 2D cases, this results in conservative posterior estimates from the classifier GP, as clearly seen from Table 3. Typically the classifier GP tends to overestimate the probability in the posterior tail area despite our attempts to change this behaviour as described in Section 2.3. While we used the Laplace approximation in our experiments, we noticed that sometimes the expectation propagation reduced the tendency to overestimate the posterior in the tails (not shown). A systematic comparison of these approximations is left for future work.

With small threshold values, such as the 0.01th quantile of the realized discrepancies, modeling the log-transformed discrepancy with a GP tends to cause too narrow posterior distributions in some scenarios, see Figure 2(e). This happens if many discrepancies are close to zero, in which case the log transformation results in a strongly skewed distribution. This may not be an issue in practice, since with many complex models simulating data such that the discrepancy becomes very small is unlikely (or impossible if the model

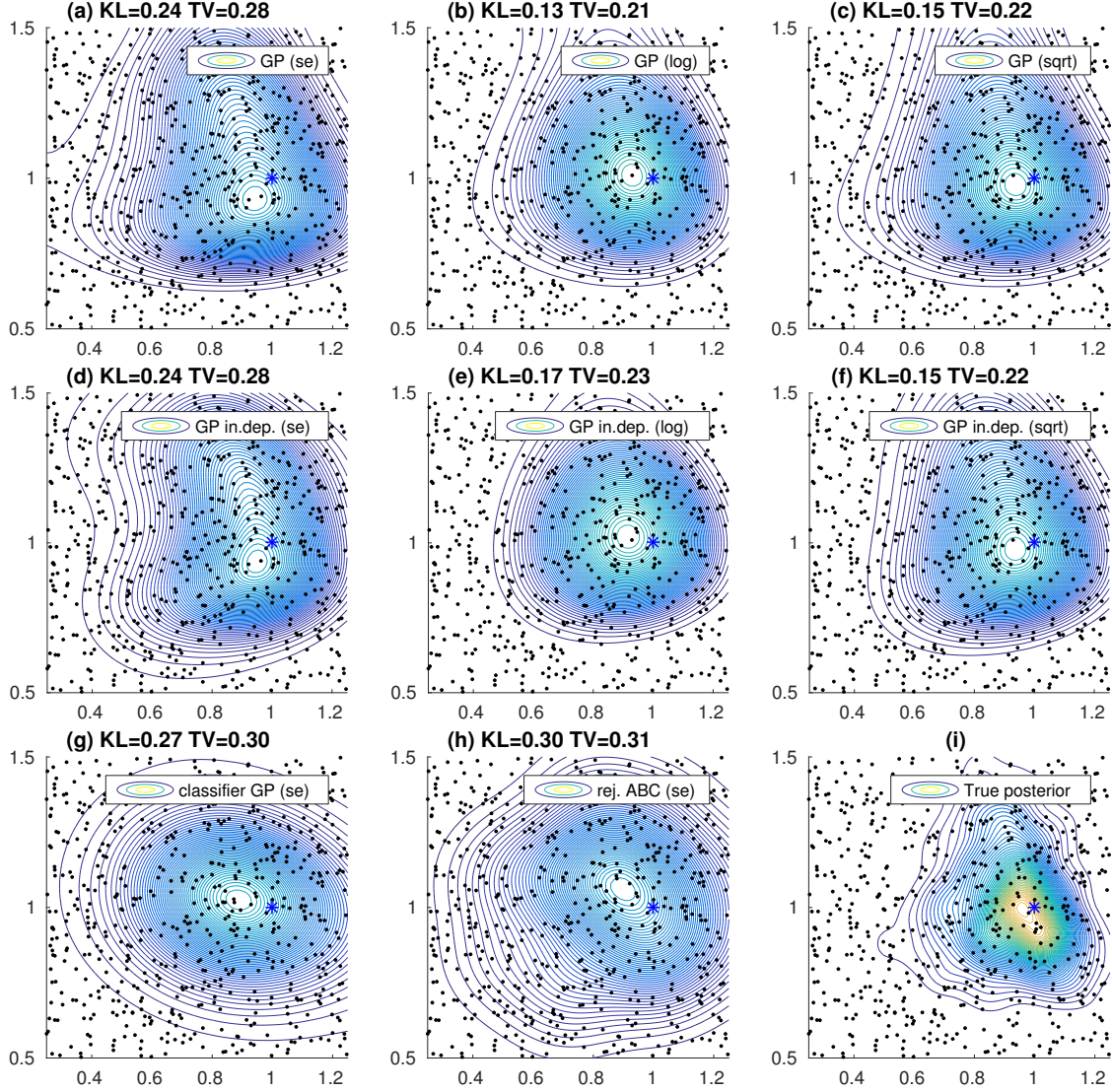


Figure 5: Posterior estimates for the Lotka-Volterra model. The black dots represent points where the simulation was run. The abbreviations 'se', 'log' and 'sqrt' refer to squared, log transformed and square-root transformed discrepancy, respectively. The parameter θ_1 is on the x-axis and θ_2 on the y-axis. With all of the methods, the uncertainty is overestimated. The difference between the standard and input-dependent GP formulations is minor, but both of them outperform the classifier GP and the rejection ABC. The log and square-root transformed discrepancies result in the most accurate approximations.

	n=50			n=100			n=200			n=400			n=600		
	se	log	sqrt	se	log	sqrt	se	log	sqrt	se	log	sqrt	se	log	sqrt
Gaussian 1:															
GP	0.14	0.13	0.08	0.12	0.13	0.07	0.12	0.12	0.06	0.12	0.13	0.04	0.13	0.12	0.04
GP in.dep.	0.25	0.20	0.10	0.21	0.19	0.09	0.23	0.16	0.07	0.22	0.15	0.05	0.23	0.15	0.04
classifier GP	0.39	0.39	0.39	0.29	0.29	0.29	0.20	0.20	0.20	0.09	0.09	0.09	0.09	0.09	0.09
rej. ABC	0.27	0.27	0.27	0.24	0.24	0.24	0.21	0.21	0.21	0.13	0.13	0.13	0.12	0.12	0.12
Bimodal:															
GP	0.23	0.49	0.16	0.22	0.24	0.12	0.22	0.17	0.09	0.22	0.15	0.08	0.22	0.14	0.07
GP in.dep.	0.17	0.61	0.19	0.19	0.41	0.13	0.20	0.27	0.10	0.20	0.23	0.08	0.21	0.21	0.07
classifier GP	0.39	0.39	0.39	0.33	0.33	0.33	0.25	0.25	0.25	0.17	0.17	0.17	0.14	0.14	0.14
rej. ABC	0.46	0.46	0.46	0.43	0.43	0.43	0.25	0.25	0.25	0.21	0.21	0.21	0.16	0.16	0.16
Gaussian 2:															
GP	0.32	0.27	0.25	0.31	0.23	0.25	0.32	0.22	0.24	0.32	0.22	0.23	0.32	0.21	0.23
GP in.dep.	0.48	0.36	0.29	0.45	0.33	0.28	0.39	0.29	0.26	0.40	0.28	0.25	0.41	0.29	0.25
classifier GP	0.36	0.36	0.36	0.31	0.31	0.31	0.24	0.24	0.24	0.18	0.18	0.18	0.16	0.16	0.16
rej. ABC	0.28	0.28	0.28	0.28	0.28	0.28	0.23	0.23	0.23	0.17	0.17	0.17	0.16	0.16	0.16
GM 1:															
GP	0.32	0.32	0.33	0.31	0.31	0.32	0.30	0.30	0.31	0.29	0.30	0.31	0.29	0.29	0.30
GP in.dep.	0.44	0.39	0.35	0.43	0.40	0.34	0.41	0.37	0.32	0.40	0.27	0.31	0.38	0.21	0.30
classifier GP	0.37	0.37	0.37	0.34	0.34	0.34	0.30	0.30	0.30	0.19	0.19	0.19	0.16	0.16	0.16
rej. ABC	0.36	0.36	0.36	0.32	0.32	0.32	0.26	0.26	0.26	0.20	0.20	0.20	0.15	0.15	0.15
GM 2:															
GP	0.22	0.15	0.15	0.20	0.13	0.14	0.20	0.13	0.13	0.21	0.13	0.13	0.21	0.13	0.13
GP in.dep.	0.25	0.19	0.15	0.23	0.17	0.13	0.23	0.16	0.13	0.23	0.16	0.12	0.24	0.16	0.12
classifier GP	0.37	0.37	0.37	0.29	0.29	0.29	0.19	0.19	0.19	0.15	0.15	0.15	0.14	0.14	0.14
rej. ABC	0.29	0.29	0.29	0.25	0.25	0.25	0.21	0.21	0.21	0.16	0.16	0.16	0.14	0.14	0.14
Uniform															
GP	0.29	0.19	0.17	0.29	0.21	0.17	0.29	0.21	0.16	0.29	0.21	0.17	0.29	0.20	0.17
GP in.dep.	0.27	0.20	0.17	0.24	0.20	0.14	0.21	0.20	0.13	0.19	0.21	0.12	0.18	0.20	0.12
classifier GP	0.43	0.43	0.43	0.34	0.34	0.34	0.23	0.23	0.23	0.12	0.12	0.12	0.11	0.11	0.11
rej. ABC	0.33	0.33	0.33	0.32	0.32	0.32	0.25	0.25	0.25	0.20	0.20	0.20	0.20	0.20	0.20
Poisson:															
GP	0.20	0.11	0.10	0.21	0.09	0.08	0.21	0.08	0.08	0.22	0.09	0.07	0.22	0.11	0.06
GP in.dep.	0.19	0.21	0.09	0.23	0.17	0.08	0.24	0.16	0.07	0.26	0.14	0.07	0.26	0.13	0.06
classifier GP	0.34	0.34	0.34	0.24	0.24	0.24	0.15	0.15	0.15	0.11	0.11	0.11	0.08	0.08	0.08
rej. ABC	0.28	0.28	0.28	0.23	0.23	0.23	0.17	0.17	0.17	0.14	0.14	0.14	0.10	0.10	0.10

Table 2: Results for the 1D toy examples. The quality of the approximation was measured using the TV distance between the estimated and the true posterior densities. The smallest TV values are bolded. Value n is the number of model simulations and 'se', 'log' and 'sqrt' refer to the squared, log-transformed and square-root-transformed discrepancies, respectively.

	n=200			n=400			n=600			n=800		
	se	log	sqrt	se	log	sqrt	se	log	sqrt	se	log	sqrt
2D Gaussian 1:												
GP	0.33	0.13	0.17	0.34	0.11	0.17	0.34	0.09	0.16	0.34	0.09	0.15
GP in.dep.	0.27	0.17	0.16	0.27	0.15	0.15	0.29	0.14	0.15	0.28	0.14	0.15
classifier GP	0.69	0.69	0.69	0.41	0.41	0.41	0.21	0.21	0.21	0.18	0.18	0.18
rej. ABC	0.34	0.34	0.34	0.29	0.29	0.29	0.26	0.26	0.26	0.25	0.25	0.25
2D Gaussian 2:												
GP	0.62	0.38	0.55	0.61	0.36	0.53	0.61	0.34	0.52	0.61	0.33	0.52
GP in.dep.	0.72	0.25	0.33	0.57	0.22	0.32	0.55	0.21	0.31	0.56	0.20	0.31
classifier GP	0.69	0.69	0.69	0.41	0.41	0.41	0.27	0.27	0.27	0.25	0.25	0.25
rej. ABC	0.38	0.38	0.38	0.36	0.36	0.36	0.33	0.33	0.33	0.30	0.30	0.30
Lotka-Volterra:												
GP	0.32	0.25	0.28	0.31	0.23	0.26	0.30	0.21	0.24	0.29	0.21	0.24
GP in.dep.	0.33	0.27	0.28	0.32	0.24	0.26	0.31	0.23	0.24	0.30	0.21	0.24
classifier GP	0.63	0.63	0.63	0.64	0.64	0.64	0.30	0.30	0.30	0.27	0.27	0.27
rej. ABC	0.35	0.35	0.35	0.33	0.33	0.33	0.31	0.31	0.31	0.29	0.29	0.29

Table 3: Results for the 2D toy examples. See the caption for Table 2 for details.

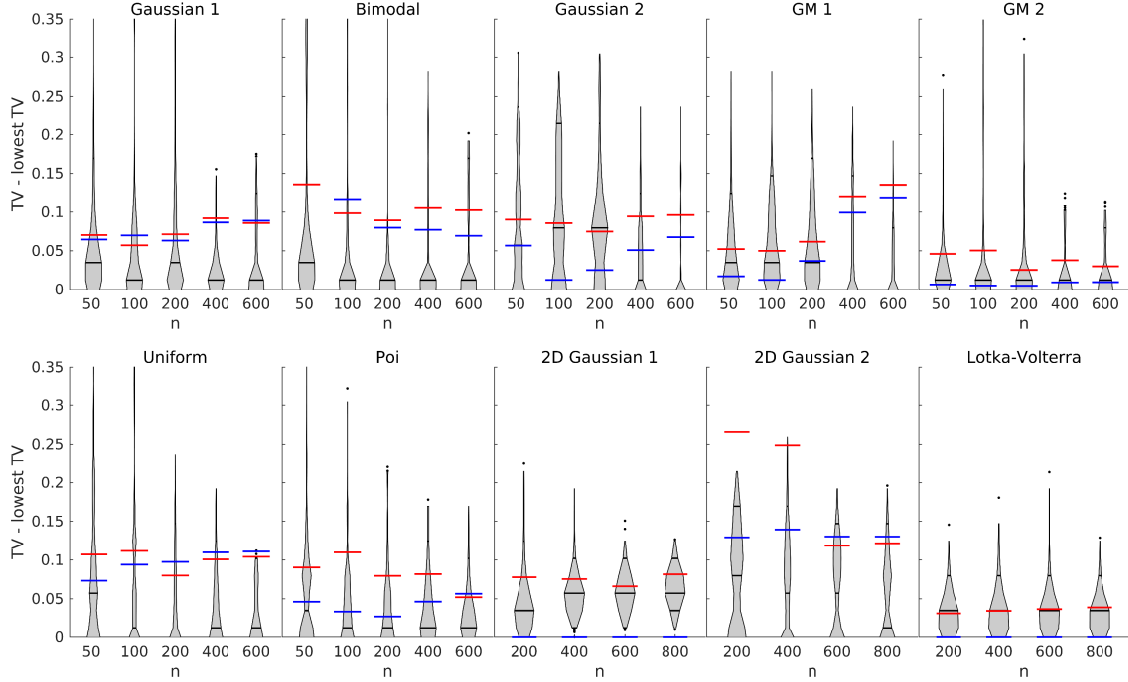


Figure 6: Results of the GP model selection using the classifier utility. We computed the TV distance between the estimated and the true posterior for all GP methods. The value on the y-axis is the difference between the TV distance of the chosen GP (corresponding to the largest utility) and the smallest TV distance observed (corresponding to the most accurate result obtainable). Therefore, the smaller the value is, the closer the selected model is to the optimal model. The violin plot shows the results over 100 different simulated data sets. The x-axis shows the number of model simulations n . The blue line represents the median results if the standard GP with the log transformation is always chosen. Another baseline shown with red is obtained by randomly selecting the GP model formulation and transformation.

is misspecified) even with the optimal parameter value. Nevertheless, according to the simulations, the log-transformation results in the best approximation in several scenarios. Especially in the 2D test problems, modeling the log-transformed discrepancy with the GPs yields the best results. A reason to this may be that the log transformation tends to underestimate the posterior variance, compensating the usual tendency of ABC to overestimate the posterior variance due to the nonzero threshold.

3.2 Model selection results

In Section 2.4, we formulated two utility functions to guide the selection of the GP model: the expected log predictive density (mlpd utility) and the expected log predictive probability of attaining a discrepancy that falls below the threshold (classifier utility). Next we illustrate the performance of these model selection criteria in practice. We consider the same toy problems as in Section 3.1. We exclude the classifier GP from the comparisons related to the mlpd utility since computing this utility requires modeling the full discrepancy distribution, whereas the classifier GP only provides an estimate of the probability of being below the threshold.

The results in Figure 6 and Figure 7 show how well the largest utilities correspond to the most accurate posterior estimates. As expected, as more simulations are available, the performance of the model selection criteria improves in most of the scenarios, such that the highest utilities better identify the GP formulation resulting in the most accurate posterior approximation. In some scenarios, there are multiple optimal GP

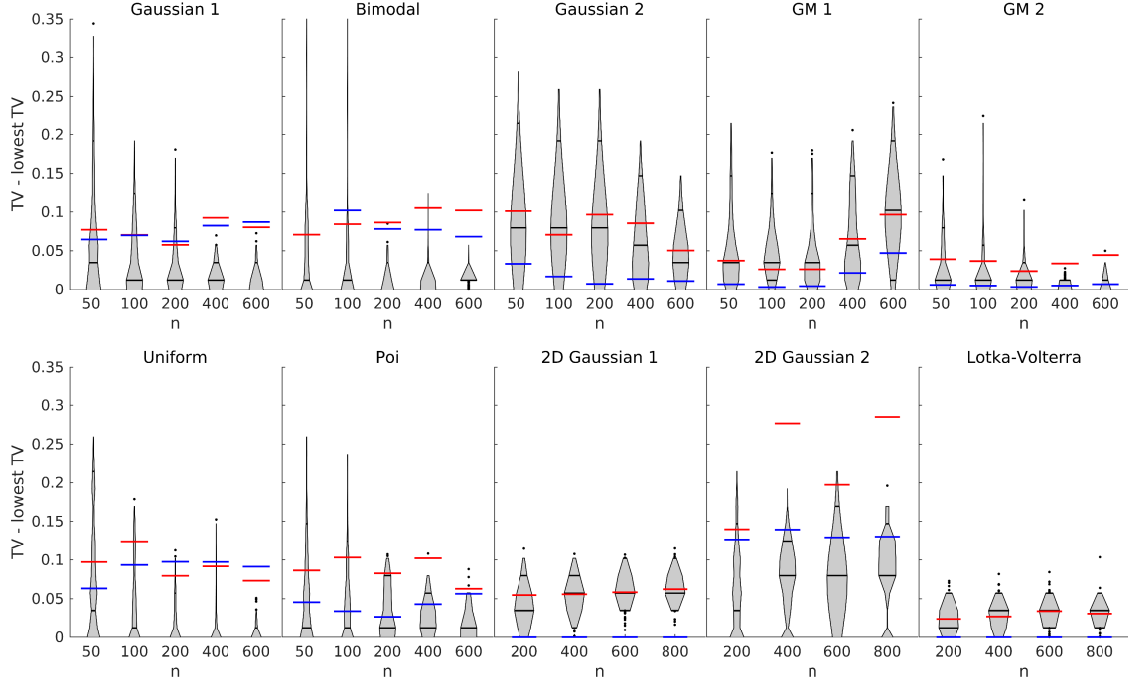


Figure 7: Results of the GP model selection for the toy examples using the mlpd utility. See the caption of the Figure 6 for an explanation.

model and/or transformation combinations, all of which are approximately equally good to one another. In these cases, it does not matter much which of the few best fitting models is selected to produce the final estimate. Despite the overall promising results, the model selection systematically fails in the case of '2D Gaussian 1' toy example. This happens because the GP model with the log transformation often underestimates the posterior uncertainty (see the corresponding one-dimensional example in Figure 2(e)), compensating the overestimation of uncertainty caused by the nonzero threshold. Consequently, it yields the best approximation to the true posterior, without having the highest utility. Furthermore, in some individual cases a GP model leading to a poor posterior approximation has the highest utility, which happens mainly with a small number of simulations and when the classifier utility is used, because then the number of cases below the threshold is very small, and consequently, the expected utility has a high variance.

Comparison of Figure 6 and Figure 7 shows that the performance difference between the two proposed utilities is relatively small, although the classifier GP can be compared to other approaches only using the classifier utility, but not with the mlpd utility. The mlpd utility is more robust with a small number of evaluations, by yielding fewer occasional bad results, but in the case of 'Gaussian 2' and 'GM 1' examples, it performs systematically worse than the classifier utility. Especially in the latter problem, even with 600 evaluations, the mlpd utility still tends to propose a suboptimal GP model. Further, the classifier utility can be used to compare basically any set of models that predict the amount of posterior mass under the threshold, making it more applicable as explained in Section 2.4. This is not the case with the mlpd utility, which requires the whole predictive distribution of the discrepancy. On the other hand, the performance of the classifier utility criterion is more dependent on the value of the threshold. If the threshold is very small, such that only a few discrepancies fall below the threshold, the method will become practically useless, contrary to the mlpd utility.

3.3 Horizontal gene transfer between bacterial genomes

The emerging field of bacterial genomics involves analysis of thousands of bacterial genomes, in order to understand the variability in bacteria as well as answer questions of practical importance, such as the spread of antibiotic resistance [Croucher et al., 2011, Chewapreecha et al., 2014]. One interesting observation is the extent to which members of the same bacterial species can differ in genome content, i.e., different strains of the same species can have different sets of genes, and only a minority of the genes is observed in all strains [Touchon et al., 2009]. Furthermore, bacteria can exchange genes with one another in a process called horizontal gene transfer (HGT) [Thomas and Nielsen, 2005]. Here we consider a previously published population genomic model that describes the variation in genome content [Marttinen et al., 2015], for which only point estimates of the parameters have previously been published, and we are interested in estimating the full posterior, when the model is fitted to a published collection of 616 genomes from *Streptococcus pneumoniae* [Croucher et al., 2013]. Briefly, the model consists of a forward-simulation of a population of bacterial strains for many generations. At each generation, the next generation is simulated by selecting strains randomly from the current generation. In addition, the genome content of the descendants may be modified by three operations, the rates of which correspond to the three parameters of the model: the gene deletion rate (*del*), novel gene introduction rate (*nov*) and HGT rate, where the gene presence-absence status of the donor strain is copied to the recipient strain (*hgt*).

To estimate the model, we consider the discrepancy

$$d^2(\theta) = w_1 \text{KL}(\theta) + w_2 (c_{\text{real}} - c_{\text{simu}}(\theta))^2,$$

where $\text{KL}(\theta)$ is the Kullback-Leibler divergence between the observed and simulated gene frequency spectra, c_{real} is the so-called observed clonality score, and $c_{\text{simu}}(\theta)$ the corresponding simulated value, see Marttinen et al. [2015] for details. The weights w_1 and w_2 are used to transform the summaries approximately on the same scale, which is common in ABC literature. Marttinen et al. [2015] achieved the same effect by log-transforming the KL-divergence, but up to this difference, the discrepancy here is the same as the one used by Marttinen et al. [2015]. Also, because the discrepancy has been investigated before, we are able to construct *a priori* plausible ranges for the parameters $\Theta = [0.01, 0.15] \times [0.1, 0.35] \times [4, 10]$, and we use the uniform prior $p(\theta) = \mathcal{U}(\Theta)$. For the GP computations the *hgt* parameter is scaled so that the parameters are approximately on the same scale. We run the simulation model in parallel with 1,000 points generated from the prior. Most simulations require one to two hours on a single computer. We set the threshold to 0.05th quantile of the simulated discrepancy values, but the 0.01th quantile led to similar conclusions. We model the discrepancy using the standard and input-dependent GP models and the same transformations as in the previous sections.

The estimated posterior is shown in Figure 8. The largest classifier utility score corresponds to the input-dependent GP model with the log transformation (classifier utility = -0.101) but also the square-root transformation with input-dependent GP and the log transformation with standard GP yield visually similar approximations with utilities -0.102 and -0.106, respectively. On the other hand, the squared discrepancy is difficult to model, resulting in overestimated posterior uncertainty (see Figure 1). In general, the input-dependent GP models have higher utilities compared to the corresponding standard GP models for this simulation model. However, since we simulate only 1,000 training data points, we expect the posterior variance to still be slightly overestimated, as seen in many toy examples. We also note that the approximated posterior agrees well with the earlier reported point estimate $\theta = (0.066, 0.18, 7.4)$. In addition, we see a strong positive correlation ($\rho = 0.47$) between the *del* and *nov* parameters, which intuitively means that a high gene deletion rate can be compensated by a high rate of introducing novel genes into the population.

Finally, we derive posterior predictive distributions for two biologically interpretable quantities, i) the ratio between the number of all gene acquisitions vs. gene deletions (computed by considering all acquisitions and deletions, whether by HGT within the population or a novel acquisition/deletion), and ii) the ratio of gene introductions to the population from outside the population (as novel genes), vs. from within the population (through HGT). The posterior predictive distributions are obtained by re-weighting the original simulations with importance sampling. The 95% credible interval for quantity i) is approximately (1.17, 1.44) and for quantity ii) it is (0.26, 0.52). Interestingly, we see that there are significantly more gene acquisitions

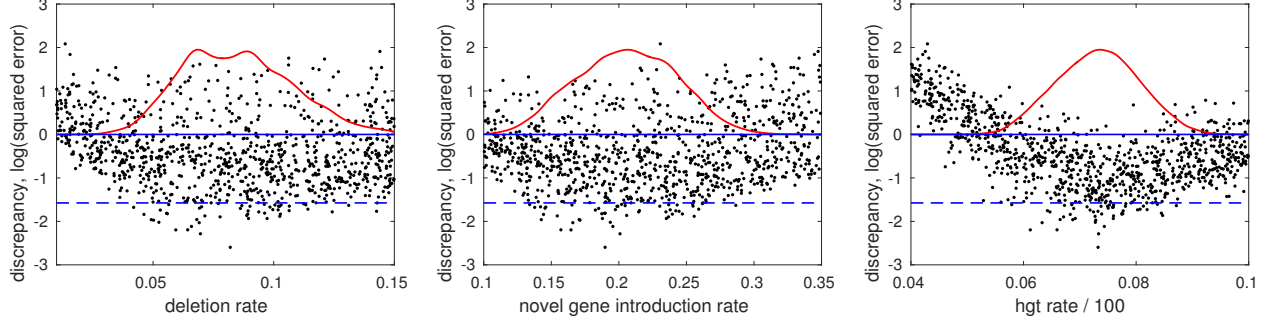


Figure 8: Marginal posterior densities for the three parameters of the genetics model. The discrepancy was log-transformed and the final model fitting was done by running the model 1000 times and using the input-dependent GP model. The black dots are the model simulations (projected to each coordinate axis), the dashed blue line is the threshold and solid blue line describes the zero line.

than deletions, as with a high probability their ratio, the quantity i), is larger than one. Because in reality the genomes are not rapidly growing, this indicates some mechanism to counter the imbalance between acquisitions and deletions, for example selection against larger genomes in general, or alternatively that many new genes are individually selected against, see discussion by Marttinen et al. [2015]. On the other hand, the ratio of gene acquisitions from outside vs. from within the population, the quantity ii), is approximately 0.4, which corresponds to the biological expectation that the majority of horizontal gene transfer events happens between closely related bacterial strains, see e.g. Majewski [2001], Fraser et al. [2007]. To our knowledge, this has not been estimated before using simulation-based inference.

4 Discussion

Many choices involved in the GP modeling were not systematically investigated. First, we only considered the squared exponential covariance function, but we expect our conclusions to hold also with other covariance functions, e.g. the Matérn, since the covariance function does not eliminate possible violations of the Gaussianity. In practice the difference between the covariance functions has been observed to be small [Jabot et al., 2014]. Second, the results also depend on the values of the GP hyperparameters, whose values we determined by maximizing the marginal likelihood. However, other approaches, such as integrating over the hyperparameters using central composite design [Rue et al., 2009], might improve the accuracy and stability, see also Snoek et al. [2012]. Third, throughout, we used relatively uninformative priors for the hyperparameters of the GP models, but set their values similarly for all problems.

In this work, we assumed the summary statistics and the discrepancy function given, but in practice they must be designed carefully. Furthermore, we considered a fixed set of transformations of the discrepancy, but other choices, such as the warped GP regression [Snelson et al., 2004], could be used to derive additional transformations. If the discrepancy is constructed from multiple summary statistics, it is possible to transform individual summaries instead of the whole discrepancy, but this requires scaling the summaries such that high variance summaries do not dominate the resulting discrepancy. Also adaptive weighting of the summaries is possible [Prangle, 2015]. Overall, the error caused by a poorly designed discrepancy may be larger than the approximation error caused by an unsuitable GP model. For example, there was little difference between the GP models and transformations in the LV example and the posterior uncertainty was inflated in all cases. Nevertheless, we find it important to understand and try to minimize the approximation error introduced in the modeling phase. As the measure of the goodness of the results, we used the total variation (TV) distance between the estimated and true posterior curves, but similar results were obtained also with the Kullback-Leibler (KL) divergence, except in some scenarios where the KL penalized heavily for the underestimation of uncertainty (exact results not shown).

We encountered occasional numerical difficulties when fitting the GP models. In particular, the input-dependent GP converged to a poor solution in a small number of experiments. An example of a difficult case is a discrepancy that is almost constant on some area of the parameter space but grows rapidly elsewhere. Also heavy tailed discrepancy distributions may cause difficulties, and, for such cases, a heavy-tailed observation model, such as the t-distribution, might be useful. Transformations, such as the log transformation, may also help. Other difficult cases include bimodal and skewed discrepancy distributions (see Example 3.3). In these difficult cases the approximation may be poor and does not improve even with additional evaluations. Despite these problems, we find that in general the BOLFI approach has a great potential for significantly improving the accuracy of the posterior approximation when the number of model evaluations is limited. On the other hand, if the dimension is low and a huge number of model evaluations is available, a more accurate posterior estimate together with convergence guarantees may be obtained by using standard ABC methods.

In order to keep focus on the GP modeling aspect, we assumed in our experiments that a region with non-negligible posterior probability was known approximately in advance. In practice, however, it has to be estimated. This can be done by Bayesian optimization with a standard GP model. While model selection may not be critical for determining the region of interest, it is an interesting future research topic to properly combine model selection with Bayesian optimization for likelihood-free inference. If the evaluation of the simulation model is computationally heavy, the sequential approach of the standard BO approach is not feasible as such, and parallel schemes, such as those recently considered by Snoek et al. [2015], González et al. [2016], are required. In principle, we could also estimate the uncertainty in the posterior density from the GP, which could provide information on the trustworthiness of the results, guide how many extra evaluations are needed for reaching a certain confidence in the result, and lead to an acquisition function tailored for posterior estimation (for example, evaluate next where the uncertainty in the posterior is largest, similar to Kandasamy, Schneider, and Póczos, 2015).

While our study is the first to compare different models for the discrepancy, other studies on modeling in ABC have been conducted before: Blum [2010] analyzed different regression adjustment methods as well as different transformations of the summary statistics when used together with a certain kernel-type estimator for partial posterior, and the author considered a leave-one-out type criterion for deciding which regression adjustment to select. We, however, consider different GP models and transformations for modeling the discrepancy. Blum [2010] also noticed that no single regression adjustment worked best and in their real-world examples they observed only small differences between the methods. We similarly observed that no single method worked best and defined a model selection criterion to choose the GP formulation. The normality assumptions of the synthetic likelihood method were examined by Price et al. [2016], and inferences were found relatively robust to deviations from normality, except when the summaries had heavy tails or were bimodal. We had similar observations when modeling the discrepancy with a GP. Jabot et al. [2014] compared different emulation methods for ABC, namely local regressions and GPs. However, unlike in this work, the authors modeled the summaries separately, as Meeds and Welling [2014], and use the emulation model inside the ABC algorithm. In addition, they considered only a single example. This is different from our work since we did not propose any sampling based ABC methods and modeled the discrepancy and not the individual summaries. Finally, Holden et al. [2015] consider and discuss certain emulation strategies focusing on climate models that have high computational cost limiting severely the budget of model simulations. However, as Wilkinson [2014], they do not model the discrepancy but the likelihood function.

We applied the GP modeling techniques to a previously published population genetic model for horizontal gene transfer in bacteria [Marttinen et al., 2015]. In this realistic example, the input-dependent GP model with log-transformed discrepancies had the highest model selection utility, and was thus selected for presenting the results. This enabled us to derive the full posterior distribution for the parameters of the model, unlike the mere point estimates published previously. Furthermore, we estimated the number of gene acquisitions to be significantly higher than the number of gene deletions, suggesting some form of selection to prevent genomes from growing rapidly, to counterbalance this observation. We also estimated for the first time using simulation-based inference the ratio of gene transfers within the population considered, and transfers from external origins, and the results supported the empirical expectation that the majority of

gene transfers happens between closely related strains. We note that multiple different models for bacterial evolution have been published, which differ in their purpose and assumptions [Fraser et al., 2007, Doroghazi and Buckley, 2011, Cohan and Perry, 2007, Shapiro et al., 2012, Ansari and Didelot, 2014, Niehus et al., 2015]. The methods considered here establish a sound basis for estimating parameters in these models and their possible future generalizations.

5 Conclusions

In this article, we examined the challenging task of approximate Bayesian computation with a small number of model evaluations, and investigated the use of Gaussian processes to model the simulated discrepancies to fully use the scarce information available. As anticipated already by Gutmann and Corander [2016], we observed that the discrepancy distribution may in realistic situations deviate from standard GP assumptions, for example the variance may be heteroscedastic or the distribution skewed or multimodal. Motivated by this, we studied various GP formulations for modeling the discrepancy, or the probability that the discrepancy is below the ABC threshold. We noticed that if the standard assumptions are violated, other models, namely the input-dependent GP and classifier GP, might produce better estimates, and suitable transformations also often improved the results. We designed a model selection criterion for choosing the GP model and transformation yielding the best estimates since no single approach performed consistently best. As discussed above, the quality of the ABC inference depends on various settings, e.g., the discrepancy, the threshold, the number of model evaluations and the strategy for selecting evaluation points. In GP-ABC, additionally the chosen GP model, its (hyper)parameters, and transformation of the discrepancy have an impact. We conclude by summarizing our findings by a few rules of thumb:

- The input-dependent GP often improves the results if the variance of the discrepancy is not constant across the parameter space. However, it involves a higher computational cost and possible instability when learning the hyperparameters.
- Focusing model simulations within the region with non-negligible posterior mass is beneficial not only because it avoids wasting computational effort for unimportant regions, but also because the resulting discrepancy distribution is easier to model using a GP. This is because the GP hyperparameters are then determined by the shape of the discrepancy distribution within the region that matters most.
- Squared or Mahalanobis-type discrepancies, e.g., $(s(x_{\text{obs}}) - s(x_{\text{simu}}))^2$, should be avoided due to their likely non-Gaussian distributions, and the dependence of the variance on the parameter, making them difficult to model with a GP. Square-root and log transformation may help.
- If a GP does not describe the shape of the discrepancy distribution well, then generating more points does not help as the model misspecification remains. In some cases none of the GP models fits the data well, leading to poor posterior approximations. In these cases the classifier GP, the smoothed ABC rejection sampler, or some more general GP formulation not investigated here might be advantageous.
- Model selection tools can be used to select GP models for approximate Bayesian computation, and their accuracy improves along with the number of model simulations available.

Acknowledgement

This work was funded by the Academy of Finland (grants no. 286607 and 294015 to PM). We acknowledge the computational resources provided by the Aalto Science-IT project.

References

M Azim Ansari and Xavier Didelot. Inference of the properties of the recombination process from whole bacterial genomes. *Genetics*, 196(1):253–265, 2014.

- M. A. Beaumont, W. Zhang, and D. J. Balding. Approximate Bayesian computation in population genetics. *Genetics*, 162(4):2025–2035, 2002.
- M. A. Beaumont, J.-M. Cornuet, J.-M. Marin, and C. P. Robert. Adaptive approximate Bayesian computation. *Biometrika*, 96(4):983–990, 2009.
- José M Bernardo and Adrian FM Smith. Bayesian theory, 2001.
- M. G. B. Blum. Approximate Bayesian Computation: a nonparametric perspective. *Journal of American Statistical Association*, 105(491):1178–1187, 2010.
- M. G. B. Blum, M. A. Nunes, D. Prangle, and S. A. Sisson. A comparative review of dimension reduction methods in approximate Bayesian computation. *Statistical Science*, 28(2):189–208, 2013.
- L. Bornn, N. S. Pillai, A. Smith, and D. Woodard. A pseudo-marginal perspective on the ABC algorithm. Available at <http://arxiv.org/abs/1404.6298v5>, 2016.
- E. Brochu, V. M. Cora, and N. de Freitas. A tutorial on Bayesian optimization of expensive cost functions, with application to active user modeling and hierarchical reinforcement learning. 2010. Available at <https://arxiv.org/abs/1012.2599>.
- C. Chewapreecha, S. R. Harris, N. J. Croucher, C. Turner, P. Marttinen, L. Cheng, A. Pessia, D. M. Aanensen, A. E. Mather, A. J. Page, et al. Dense genomic sampling identifies highways of pneumococcal recombination. *Nature Genetics*, 46(3):305–309, 2014.
- F. M. Cohan and E. B. Perry. A systematics for discovering the fundamental units of bacterial diversity. *Current Biology*, 17(10):R373–R386, 2007.
- N. J. Croucher, S. R. Harris, C. Fraser, M. A. Quail, J. Burton, M. van der Linden, L. McGee, A. von Gottberg, J. H. Song, K. S. Ko, et al. Rapid pneumococcal evolution in response to clinical interventions. *Science*, 331(6016):430–434, 2011.
- N. J. Croucher, J. A. Finkelstein, S. I. Pelton, P. K. Mitchell, G. M. Lee, J. Parkhill, S. D. Bentley, W. P. Hanage, and M. Lipsitch. Population genomics of post-vaccine changes in pneumococcal epidemiology. *Nature Genetics*, 45(6):656–663, 2013.
- J. R. Doroghazi and D. H. Buckley. A model for the effect of homologous recombination on microbial diversification. *Genome biology and evolution*, 3:1349–1356, 2011.
- C. C. Drovandi, M. T. Moores, and R. J. Boys. Accelerating pseudo-marginal MCMC using Gaussian processes. Available at <http://eprints.qut.edu.au/90973/>. Online. Accessed 19-10-2016, 2015a.
- C. C. Drovandi, A. N. Pettitt, and A. Lee. Bayesian indirect inference using a parametric auxiliary model. *Statistical Science*, 30(1):72–95, 2015b.
- Y. Fan, D. J. Nott, and S. A. Sisson. Approximate Bayesian computation via regression density estimation. *Stat*, 2(1):34–48, 2013.
- P. Fearnhead and D. Prangle. Constructing summary statistics for approximate Bayesian computation: Semi-automatic approximate Bayesian computation. *Journal of the Royal Statistical Society. Series B: Statistical Methodology*, 74(3):419–474, 2012.
- C. Fraser, W. P. Hanage, and B. G. Spratt. Recombination and the nature of bacterial speciation. *Science*, 315(5811):476–480, 2007.
- P. W. Goldberg, C. K. I. Williams, and C. M. Bishop. Regression with input-dependent noise: A Gaussian process treatment. *Advances in Neural Information Processing Systems*, 10:493–499, 1997.

- J. González, M. Osborne, and N. D. Lawrence. GLASSES: Relieving The Myopia Of Bayesian Optimisation. In *Proceedings of the Nineteenth International Workshop on Artificial Intelligence and Statistics*, 2016.
- M. U. Gutmann and J. Corander. Bayesian optimization for likelihood-free inference of simulator-based statistical models. *Journal of Machine Learning Research*, 17(125):1–47, 2016.
- F. Hartig, J. M. Calabrese, B. Reineking, T. Wiegand, and A. Huth. Statistical inference for stochastic simulation models—theory and application. *Ecology Letters*, 14(8):816–27, 2011.
- P. Holden, N. Edwards, J. Hensman, and R. D. Wilkinson. ABC for climate: dealing with expensive simulators. In *To appear in the Handbook of ABC*. 2015. Available at <http://arxiv.org/abs/1511.03475>.
- F. Jabot, G. Lagarrigues, B. Courbaud, and N. Dumoulin. A comparison of emulation methods for Approximate Bayesian Computation. Available at <http://arxiv.org/abs/1412.7560>, 2014.
- K. Kandasamy, J. Schneider, and B. Póczos. Bayesian active learning for posterior estimation. In *International Joint Conference on Artificial Intelligence*, pages 3605–3611, 2015.
- M. Lenormand, F. Jabot, and G. Deffuant. Adaptive approximate Bayesian computation for complex models. *Computational Statistics*, 28(6):2777–2796, 2013.
- J. Majewski. Sexual isolation in bacteria. *FEMS Microbiology Letters*, 199(2):161–169, 2001.
- J. M. Marin, P. Pudlo, C. P. Robert, and R. J. Ryder. Approximate Bayesian computational methods. *Statistics and Computing*, 22(6):1167–1180, 2012.
- P. Marjoram, J. Molitor, V. Plagnol, and S. Tavaré. Markov chain Monte Carlo without likelihoods. *Proceedings of the National Academy of Sciences of the United States of America*, 100(26):15324–8, 2003.
- P. Marttinen, M. U. Gutmann, N. J. Croucher, W. P. Hanage, and J. Corander. Recombination produces coherent bacterial species clusters in both core and accessory genomes. *Microbial Genomics*, 1(5), 2015.
- E. Meeds and M. Welling. GPS-ABC: Gaussian Process Surrogate Approximate Bayesian Computation. In *Proceedings of the 30th Conference on Uncertainty in Artificial Intelligence*, 2014.
- P. Moral, A. Doucet, and A. Jasra. An adaptive sequential Monte Carlo method for approximate Bayesian computation. *Statistics and Computing*, 22(5):1009–1020, 2012.
- R. Niehus, S. Mitri, A. G. Fletcher, and K. R. Foster. Migration and horizontal gene transfer divide microbial genomes into multiple niches. *Nature Communications*, 6, 2015.
- D. Prangle. Adapting the ABC distance function. Available at <http://arxiv.org/abs/1507.00874>, 2015.
- L. F. Price, C. C. Drovandi, A. Lee, and D. J. Nott. Bayesian synthetic likelihood. Available at <http://eprints.qut.edu.au/92795/> Online. Accessed 19-10-2016, 2016.
- C. E. Rasmussen and C. K. I. Williams. *Gaussian Processes for Machine Learning*. The MIT Press, 2006.
- H. Rue, S. Martino, and N. Chopin. Approximate Bayesian inference for latent Gaussian models by using integrated nested Laplace approximations. *Journal of the Royal Statistical Society. Series B: Statistical Methodology*, 71(2):319–392, 2009.
- B. Shahriari, K. Swersky, Z. Wang, R. P. Adams, and N. de Freitas. Taking the human out of the loop: A review of Bayesian optimization. *Proceedings of the IEEE*, 104(1), 2015.
- B. J. Shapiro, J. Friedman, O. X. Cordero, S. P. Preheim, S. C. Timberlake, G. Szabó, M. F. Polz, and E. J. Alm. Population genomics of early events in the ecological differentiation of bacteria. *Science*, 336(6077):48–51, 2012.

- S. A. Sisson, Y. Fan, and M. M. Tanaka. Sequential Monte Carlo without likelihoods. *Proceedings of the National Academy of Sciences of the United States of America*, 104(6):1760–5, 2007.
- E. Snelson, C. E. Rasmussen, and Z. Ghahramani. Warped Gaussian processes. In *Advances in Neural Information Processing Systems 16*, pages 337–344, 2004.
- J. Snoek, O. Rippel, K. Swersky, R. Kiros, N. Satish, N. Sundaram, M. Patwary, M. Ali, and R. P. Adams. Scalable Bayesian optimization using deep neural networks. In *International Conference on Machine Learning*, 2015.
- Jasper Snoek, Hugo Larochelle, and Ryan P Adams. Practical Bayesian optimization of machine learning algorithms. In *Advances in Neural Information Processing Systems 25*, pages 1–9, 2012.
- C. M. Thomas and K. M. Nielsen. Mechanisms of, and barriers to, horizontal gene transfer between bacteria. *Nature Reviews Microbiology*, 3(9):711–721, 2005.
- V. Tolvanen, P. Jylänki, and A. Vehtari. Approximate inference for nonstationary heteroscedastic Gaussian process regression. In *2014 IEEE International Workshop on Machine Learning for Signal Processing*, pages 1–24, 2014.
- T. Toni, D. Welch, N. Strelkowa, A. Ipsen, and M. P. H. Stumpf. Approximate Bayesian computation scheme for parameter inference and model selection in dynamical systems. *Journal of the Royal Society, Interface*, 6(31):187–202, 2009.
- M. Touchon, C. Hoede, O. Tenaillon, V. Barbe, S. Baeriswyl, P. Bidet, E. Bingen, S. Bonacorsi, C. Bouchier, O. Bouvet, et al. Organised genome dynamics in the escherichia coli species results in highly diverse adaptive paths. *PLoS Genetics*, 5(1):e1000344, 2009.
- B. M. Turner and P. B. Sederberg. A generalized, likelihood-free method for posterior estimation. *Psychonomic Bulletin & Review*, 21(2):227–250, 2014.
- B. M. Turner and T. Van Zandt. A tutorial on approximate Bayesian computation. *Journal of Mathematical Psychology*, 56(2):69–85, 2012.
- J. Vanhatalo, J. Riihimäki, J. Hartikainen, P. Jylänki, V. Tolvanen, and A. Vehtari. GPstuff: Bayesian modeling with Gaussian processes. *Journal of Machine Learning Research*, 14:1175–1179, 2013.
- A. Vehtari and J. Lampinen. Bayesian model assessment and comparison using cross-validation predictive densities. *Neural computation*, 14(10):2439–2468, 2002.
- R. D. Wilkinson. Approximate Bayesian computation (ABC) gives exact results under the assumption of model error. *Statistical Applications in Genetics and Molecular Biology*, 12(2):129–141, 2013.
- R. D. Wilkinson. Accelerating ABC methods using Gaussian processes. In *Proceedings of the Seventeenth International Conference on Artificial Intelligence and Statistics*, pages 1015–1023, 2014.
- S. N. Wood. Statistical inference for noisy nonlinear ecological dynamic systems. *Nature*, 466:1102–1104, 2010.